Geometric finite difference schemes for the generalized hyperelastic-rod wave equation

David Cohen[a,*], Xavier Raynaud[b]

[a] *Mathematisches Institut, Universität Basel, CH-4051 Basel, Switzerland. Email: David.Cohen@unibas.ch*

[b] *Center of Mathematics for Applications, University of Oslo, NO–0316 Oslo, Norway. Email: xavierra@cas.uio.no*

Abstract

Geometric integrators are presented for a class of nonlinear dispersive equations which includes the Camassa-Holm equation, the BBM equation and the hyperelastic-rod wave equation. One group of schemes is designed to preserve a global property of the equations: the conservation of energy; while the other one preserves a more local feature of the equations: the multi-symplecticity.

Keywords: Hyperelastic-rod wave, Camassa–Holm equation, BBM equation, Conservative schemes, Finite Difference, Discrete gradients, Multi-symplecticity, Euler box scheme.

1. Introduction

We consider the generalized hyperelastic-rod wave equation

$$u_t - u_{xxt} + \frac{1}{2}g(u)_x - \gamma(2u_x u_{xx} + u u_{xxx}) = 0, \quad u|_{t=0} = u_0, \tag{1}$$

with periodic boundary conditions and where $u = u(t,x)$ and g is a given smooth function. The generalized hyperelastic-rod wave equation was first introduced in [1] where the global existence of the dissipative solutions is established. For the proof of the existence of the global and conservative solutions, we refer to [2].

The problem (1) defines a whole class of equations, depending on the function g and the value of γ, which contains several well-known nonlinear dispersive equations.

*

Taking $\gamma = 1$ and $g(u) = 2\kappa u + 3u^2$ (with $\kappa \geq 0$), equation (1) reduces to the Camassa–Holm equation:

$$u_t - u_{xxt} + \kappa u_x + 3uu_x - 2u_x u_{xx} - uu_{xxx} = 0. \tag{2}$$

Since its introduction in [3] in the context of water wave propagation where u represents the height's free surface above a flat bottom while κ is a parameter, the Camassa–Holm equation has been extensively studied, mainly because of its rich mathematical structure. The Camassa–Holm equation possesses a Lax pair which allows for a scattering and inverse scattering analysis, showing that the equation is integrable ([3, 4, 5, 6]). It is a geodesic on the group of diffeomorphisms for a given metric ([7, 8]). In addition, the Camassa–Holm equation is bi-Hamiltonian (see Section 2 for definitions and references). The bi-Hamiltonian structure of the equation will be used in this article to derive energy preserving numerical schemes (see Section 3). For $g(u) = 3u^2$, equation (1) becomes the hyperelastic-rod wave equation:

$$u_t - u_{xxt} + 3uu_x - \gamma(2u_x u_{xx} + uu_{xxx}) = 0, \tag{3}$$

which was introduced by Dai [9] in 1998. This equation models the propagation of nonlinear waves in cylindrical axially symmetric hyperelastic-rod. The parameter $\gamma \in \mathbb{R}$ is a constant depending on the material and pre-stress of the rod. The well-posedness of the Cauchy problem for (3) is established in [10, 11]. For $g(u) = 2u + u^2$ and for $\gamma = 0$, equation (1) leads to the Benjamin-Bona-Mahony (BBM) equation (or regularized long wave) [12]:

$$u_t - u_{xxt} + u_x + uu_x = 0, \tag{4}$$

which describes surface wave in a channel. While the solutions of the BBM equation are unique and globally defined in time, the solutions of the Camassa–Holm and hyperelastic-rod wave equations may break down in finite time. Due to the particular circumstances in which this occurs, this situation is also referred as wave breaking (see [13, 14] for more details). After wave breaking, the solutions are no longer unique and, in this article, only solutions before wave breaking will be considered.

We now briefly review – without intending to be exhaustive – the numerical schemes related to the generalized hyperelastic-rod wave equation that can be found in the literature. For the Camassa–Holm equation, schemes using pseudo-spectral discretization have been used in [15, 16]. Methods based on multipeakons, a special class of solutions of the Camassa–Holm equation, can be found in [17, 18, 19, 20]. Finite difference schemes with convergence proof are studied in [21, 22]. In [23], the authors use a finite element method to derive a scheme which is high order accurate

and nonlinearly stable. The Camassa–Holm equation admits a multi-symplectic formulation which can be used to derive multi-symplectic numerical schemes, see [24]. For the BBM equation, conservative finite difference schemes were proposed in [25] with a convergence and stability analysis. We also refer to [26, 27]. As far as the hyperelastic-rod wave equation, the authors are only aware of the numerical scheme given in [28] which is based on a Galerkin approximation and preserves a discretization of the energy.

In this article we derive finite difference schemes for the generalized hyperelastic-rod equation which preserve some of the geometric properties of the equation. The first property is a global one, namely the preservation of the energy, while the second is local and corresponds to the preservation of multi-symplecticity. In Section 2, we look at the Hamiltonian formulations of (1) and explain how methods for ordinary differential equations based on discrete gradients that have been developed in [29] can be applied to equation (1). In Section 3, the discrete gradients are computed and the corresponding energy preserving schemes are derived. The discrete gradient method is also applied to the hyperelastic-rod wave equation in [28] (in a Galerkin setting) and to related partial differential equations in [30, 31]. Our discrete gradient schemes are based on the Hamiltonian formulations of the equation and we introduce a discrete product rule for differentiation which allows for a simple calculation of the discrete derivative of the two Hamiltonians we are considering. In Section 4, we review some of the general theory of multi-symplectic PDEs following the approach of Bridges and Reich [32] and based on the work in [24], we derive a multi-symplectic scheme for the generalized hyperelastic-rod wave equation (1). Finally, we illustrate the behavior of these new schemes by numerical experiments in Section 5.

2. The discrete gradient approach

In this section we review the Hamiltonian formulation for partial differential equations, give the Hamiltonian formulations for the equations we are considering and finally present the discrete gradient methods for ODEs of [29]. We also refer to [33], where the author sets up the formalism of the discrete gradient.

We first consider the Camassa–Holm equation (2) in the limiting case $\kappa = 0$:

$$u_t - u_{xxt} + 3uu_x - 2u_x u_{xx} - uu_{xxx} = 0.$$

Defining $m = u - u_{xx}$, this equation can be rewritten as a Hamiltonian partial differential equation, that is,

$$m_t = \mathcal{D}(m)\frac{\delta \mathcal{H}}{\delta m}, \tag{5}$$

where the functional $\mathcal{H}(m)$ is the Hamiltonian and $\frac{\delta \mathcal{H}}{\delta m}$ denotes the variational derivative of $\mathcal{H}$ with respect to m defined as

$$\left\langle \frac{\delta \mathcal{H}}{\delta m}, \tilde{m} \right\rangle_{L^2} = \frac{d}{d\varepsilon}\Big|_{\varepsilon=0} \mathcal{H}(m+\varepsilon\tilde{m}) \quad \text{for all } \tilde{m}$$

(here $\langle v, w\rangle_{L^2} = \int v(x)w(x)\,\mathrm{d}x$ denotes the L^2-scalar product). Equation (5) defines a Hamiltonian equation if in addition the operator $\mathcal{D}(m)$ is antisymmetric with respect to the L^2-scalar product, that is,

$$\langle v, \mathcal{D}(m)w\rangle_{L^2} = -\langle \mathcal{D}(m)v, w\rangle_{L^2},$$

and its Poisson bracket

$$\{F, H\}(m) = \left\langle \frac{\delta F}{\delta m}, \mathcal{D}(m)\frac{\delta H}{\delta m} \right\rangle_{L^2}$$

satisfies the Jacobi identity

$$\{\{F, G\}, H\} + \{\{G, H\}, F\} + \{\{H, F\}, G\} = 0. \tag{6}$$

The Camassa-Holm equation with $\kappa = 0$ has a bi-Hamiltonian structure (see [34] for the definition and [3, 35] for the proofs): It is Hamiltonian for the two following pairs of antisymmetric operator and Hamiltonian function,

$$\begin{aligned} \mathcal{D}_1(m)(v) &= -mv_x - (mv)_x = -(u - u_{xx})v_x - ((u - u_{xx})v)_x, \\ \mathcal{H}_1(m) &= \frac{1}{2}\int (u^2 + u_x^2)\,\mathrm{d}x \end{aligned} \tag{7}$$

and

$$\begin{aligned} \mathcal{D}_2(m)(v) &= -(\partial_x(1 - \partial_{xx}))v, \\ \mathcal{H}_2(m) &= \frac{1}{2}\int (u^3 + uu_x^2)\,\mathrm{d}x, \end{aligned} \tag{8}$$

where the operators $\mathcal{D}_1$ and $\mathcal{D}_2$, evaluated at the point m, are applied to a function v. For the other partial differential equations considered in the introduction, it is not clear if they also possess a bi-Hamiltonian structure (the issue here being the Jacobi identity (6)), nevertheless we have the following Hamiltonian formulations. Firstly we not that the analogous $\mathcal{D}_2(m)$ formulations of the equations are Hamiltonian (this is because this operator is skew-symmetric and independent of m) and that the analogous $\mathcal{D}_1(m)$ formulations are (at least) skew-symmetric. For the hyperelastic-rod wave equation (3), there exists, at least, two functionals $\mathcal{H}_1(m)$ and $\mathcal{H}_2(m)$

($\mathcal{H}_1(m)$ corresponds to the energy of the problem), and two antisymmetric operators $\mathcal{D}_1(m)$ and $\mathcal{D}_2(m)$ such that this equation can be written as a Hamiltonian problem as in (5). They are given by

$$\begin{aligned}\mathcal{D}_1(m)(v) &= -(u-\gamma u_{xx})v_x - ((u-\gamma u_{xx})v)_x,\\ \mathcal{H}_1(m) &= \frac{1}{2}\int (u^2+u_x^2)\,\mathrm{d}x\end{aligned} \tag{9}$$

and

$$\begin{aligned}\mathcal{D}_2(m)(v) &= -(\partial_x(1-\partial_{xx}))v,\\ \mathcal{H}_2(m) &= \frac{1}{2}\int (u^3+\gamma u u_x^2)\,\mathrm{d}x,\end{aligned} \tag{10}$$

where, as before, we have $u=(1-\partial_{xx})^{-1}m$. For the Camassa–Holm equation given by (2), we obtain

$$\begin{aligned}\mathcal{D}_1(m)(v) &= -(u-u_{xx}+\tfrac{\kappa}{2})v_x - ((u-u_{xx}+\tfrac{\kappa}{2})v)_x,\\ \mathcal{H}_1[m] &= \frac{1}{2}\int (u^2+u_x^2)\,\mathrm{d}x\end{aligned} \tag{11}$$

and

$$\begin{aligned}\mathcal{D}_2(m)(v) &= -(\partial_x(1-\partial_{xx}))v,\\ \mathcal{H}_2[m] &= \frac{1}{2}\int (u^3+\kappa u^2+u u_x^2)\,\mathrm{d}x.\end{aligned} \tag{12}$$

We note that the Camassa–Holm equation (2) has also a bi-Hamiltonian structure, the proof of this fact follows the lines of [35].

For the generalized hyperelastic-rod wave equation (1), the formulation equivalent to (9) is not available and we only have the Hamiltonian formulation given by

$$\begin{aligned}\mathcal{D}_2(m)(v) &= -(\partial_x(1-\partial_{xx}))v,\\ \mathcal{H}_2(m) &= \frac{1}{2}\int (G(u)+\gamma u u_x^2)\,\mathrm{d}x,\end{aligned} \tag{13}$$

where G is an integral of g, i.e., $G'=g$. Finally, for the BBM equation (4), we have

$$\begin{aligned}\mathcal{D}_1(m)(v) &= -(\tfrac{u}{3}+\tfrac{1}{2})v_x - ((\tfrac{u}{3}+\tfrac{1}{2})v)_x,\\ \mathcal{H}_1(m) &= \frac{1}{2}\int (u^2+u_x^2)\,\mathrm{d}x,\end{aligned} \tag{14}$$

and

$$\mathcal{D}_2(m)(v) = -(\partial_x(1-\partial_{xx}))v,$$
$$\mathcal{H}_2(m) = \frac{1}{2}\int (u^2 + \frac{u^3}{3})\,\mathrm{d}x. \tag{15}$$

A remarkable feature of a Hamiltonian partial differential equation is the fact that the Hamiltonian functional $\mathcal{H}$ is conserved along the exact solution of the problem. Indeed, we have

$$\frac{\mathrm{d}\mathcal{H}}{\mathrm{d}t} = \left\langle \frac{\delta\mathcal{H}}{\delta m}, \frac{\mathrm{d}m}{\mathrm{d}t}\right\rangle = \left\langle \frac{\delta\mathcal{H}}{\delta m}, \mathcal{D}(m)\frac{\delta\mathcal{H}}{\delta m}\right\rangle = 0, \tag{16}$$

using the fact that the operator $\mathcal{D}(m)$ is antisymmetric. The Hamiltonians $\mathcal{H}_1$ and $\mathcal{H}_2$ are thus conserved along the exact solution of the partial differential equations considered here. Our goal in the next section will be to exploit this feature of the exact solution to design numerical schemes that exactly preserve a discretized version of these Hamiltonians. To do so, we first have to find appropriate discretizations of the partial differential equations (see Section 3 for the details) and then integrate the obtained differential equations in time by the *discrete gradient* approach.

We now review the discrete gradient approach used in the numerical integration of ODEs proposed in [29] (see also references therein). For a given smooth function $H : \mathbb{R}^n \to \mathbb{R}$ and a skew-symmetric matrix $D(y)$ depending on y, we consider the differential equation in $\mathbb{R}^n$ given by

$$\dot{y} = f(y) = D(y)\nabla H(y). \tag{17}$$

We say that $\overline{\nabla} H$ is a *discrete gradient* of H if

$$H(y') - H(y) = \overline{\nabla} H(y, y') \cdot (y' - y) \quad \text{for all } y, y' \in \mathbb{R}^n \tag{18}$$

and the consistency relation $\overline{\nabla} H(y, y) = \nabla H(y)$ is satisfied. Given a discrete gradient $\overline{\nabla} H$, one can construct schemes of the form

$$\frac{y_{n+1} - y_n}{\Delta t} = \tilde{D}(y_n, y_{n+1}, \Delta t)\overline{\nabla} H(y_n, y_{n+1}), \tag{19}$$

where we impose that the operator $v \mapsto \tilde{D}(y, y', \Delta t)(v)$ is antisymmetric for all $y, y', \Delta t$ and, for consistency reason, $\tilde{D}(y, y, 0) = D(y)$. There exist several discrete gradients of the same function H and one of them is given by the *mean value discrete gradient*, see [36, 29], which is given by

$$\overline{\nabla} H(y_n, y_{n+1}) = \int_0^1 \nabla H((1-\zeta)y_n + \zeta y_{n+1})\mathrm{d}\zeta. \tag{20}$$

In the next section, we will introduce another discrete gradient which can be applied to the type of Hamiltonians we will be considering.

Schemes which take the form (19) exactly preserve the value of $H(y_n)$, as we have

$$\begin{aligned} H(y_{n+1}) - H(y_n) &= \overline{\nabla} H(y_n, y_{n+1}) \cdot (y_{n+1} - y_n) \\ &= \Delta t \overline{\nabla} H(y_n, y_{n+1}) \cdot \tilde{D}(y_n, y_{n+1}, \Delta t) \overline{\nabla} H(y_n, y_{n+1}) = 0. \end{aligned} \tag{21}$$

3. Energy preserving schemes

We consider periodic solutions on the interval $[0, T]$. We introduce the partition of $[0, T]$ in points separated by a distance $\Delta x = 1/n$ denoted $x_i = i\Delta x$ for $i = 0, \ldots, n-1$. We consider the time step discretization step Δt and $t_j = j\Delta t$. At $x = x_i$ and $t = t_j$, the value of u is approximated by u_i^j. We define the right and left discrete derivatives with respect to space at (x_i, t_j) as

$$(\delta_x^{\pm} u)_i^j = \frac{\pm 1}{\Delta x}(u_{i\pm 1}^j - u_i^j)$$

and the symmetric derivative as

$$\delta_x = \frac{1}{2}(\delta_x^+ + \delta_x^-).$$

For the rest of this section, we also define the following compact discrete operator

$$\delta_x^2 = \delta_x^+ \delta_x^- = \delta_x^- \delta_x^+.$$

In order to derive energy-preserving schemes, we have to define all the continuous operations at the discrete level. The L^2-scalar product in the continuous case becomes the following discrete one

$$\langle u, v \rangle = \Delta x \sum_{i=0}^{n-1} u_i v_i \tag{22}$$

for which the following discrete summation by part rules hold:

$$\left\langle \delta_x^{\pm} u, v \right\rangle = -\left\langle u, \delta_x^{\mp} v \right\rangle \text{ and } \left\langle \delta_x u, v \right\rangle = -\left\langle u, \delta_x v \right\rangle. \tag{23}$$

We have to discretize the Hamiltonians $\mathcal{H}_1$ and $\mathcal{H}_2$. We will only consider in details the hyperelastic-rod wave equation, the results for the other equations being listed below. Let us now define $m = (1 - \delta_x^2)u$, we approximate $\mathcal{H}_1$ and $\mathcal{H}_2$ by

$$H_1(m) = \frac{\Delta x}{2} \sum_{i=0}^{n-1} \left((u_i)^2 + (\delta_x^+ u_i)^2 \right) \tag{24}$$

and

$$H_2(m) = \frac{\Delta x}{2} \sum_{i=0}^{n-1} \big((u_i)^3 + \gamma u_i \delta_x^+ u_i \delta_x^- u_i\big), \tag{25}$$

respectively. Here, we could have chosen in the definition of the Hamiltonians the symmetric discrete derivative δ_x and we would have obtained $H_1(m) = \frac{\Delta x}{2} \sum_{i=0}^{n-1} \big((u_i)^2 + (\delta_x u_i)^2\big)$ and $H_2(m) = \frac{\Delta x}{2} \sum_{i=0}^{n-1} \big((u_i)^3 + \gamma u_i (\delta_x u_i)^2\big)$. However, this choice leads to the use of the non compact discrete operator $\delta_x \delta_x$ which may cause instability[1], see e.g [37].

Several methods to compute discrete gradients are given in [29]. In this section, we present another method which can be used in the case where the Hamiltonians consist only of sums and products of the unknown variables (i.e. $\{u_i\}_{i=0}^{n-1}$), as in (24) and (25). For a scalar function f, we denote the difference $f(m') - f(m)$ by $\delta[f]$ and the average $\frac{f(m')+f(m)}{2}$ by $\mu[f]$. A straightforward computation shows that, for any m and m', we have

$$f(m')g(m') - f(m)g(m) = \frac{1}{2}(f(m') - f(m))(g(m') + g(m)) + \frac{1}{2}(g(m') - g(m))(f(m') + f(m))$$

which rewrites with our new notation as

$$\delta[(f \cdot g)] = \delta[f] \cdot \mu[g] + \delta[g] \cdot \mu[f]. \tag{26}$$

Note the similarity between (26) and the Leibniz rule $(fg)' = f'g + g'f$ and it becomes clear that the operator μ is introduced to account for the failure of a simple difference to fulfill the Leibniz rule. By recursively applying the product rule (26), we obtain

$$\begin{aligned} \delta[H_1] &= \frac{\Delta x}{2} \sum_{i=0}^{n-1} \delta[(u_i)^2 + (\delta_x^+ u_i)^2] \\ &= \frac{\Delta x}{2} \sum_{i=0}^{n-1} (2\delta[u_i]\mu[u_i] + 2\delta[\delta_x^+ u_i]\mu[\delta_x^+ u_i]). \end{aligned}$$

We use the fact that δ and μ commute with $\delta_x^\pm$ (which follows from the linearity of

[1] We thank the referee for pointing this out.

δ), the summation by part rule, and we obtain

$$\begin{aligned}\delta[H_1] &= \Delta x \sum_{i=0}^{n-1} (\delta[u_i]\mu[u_i] - \mu[u_i]\delta[\delta_x^2 u_i]) \\ &= \Delta x \sum_{i=0}^{n-1} \mu[u_i](\delta[u_i] - \delta[\delta_x^2 u_i]) \\ &= \langle \mu[u], \delta[m] \rangle ,\end{aligned}$$

by the definition of the discrete scalar product (22). Hence, using the fact that $m = (1-\delta_x^2)u$, we get

$$H_1(m') - H_1(m) = \langle \mu[u], \delta[m] \rangle = \left\langle \frac{u'+u}{2}, m'-m \right\rangle \tag{27}$$

and the discrete gradient of H is given in this case by

$$\overline{\nabla} H_1(m,m') = \mu[u] = \frac{u+u'}{2} = (1-\delta_x^2)^{-1}\left(\frac{m+m'}{2}\right). \tag{28}$$

For the second Hamiltonian of the hyperelastic-rod wave equation given by (25), we obtain

$$\begin{aligned}\delta[H_2] &= \frac{\Delta x}{2} \sum_{i=0}^{n-1} \delta[(u_i)^3 + \gamma u_i \delta_x^+ u_i \delta_x^- u_i] \\ &= \frac{\Delta x}{2} \sum_{i=0}^{n-1} (\mu[(u_i)^2]\delta[u_i] + \mu[u_i]\delta[(u_i)^2] + \gamma\delta[u_i]\mu[\delta_x^+ u_i \delta_x^- u_i] + \gamma\mu[u_i]\delta[\delta_x^+ u_i \delta_x^- u_i]) \\ &= \frac{\Delta x}{2} \sum_{i=0}^{n-1} \left(\left(\mu[(u_i)^2] + 2\mu[u_i]^2 + \gamma\mu[\delta_x^+ u_i \delta_x^- u_i] \right) \delta[u_i] + \gamma\mu[u_i]\delta[\delta_x^+ u_i \delta_x^- u_i] \right) \\ &= \frac{\Delta x}{2} \sum_{i=0}^{n-1} \Big(\mu[(u_i)^2] + 2\mu[u_i]^2 + \gamma\mu[\delta_x^+ u_i \delta_x^- u_i] - \gamma\delta_x^-(\mu[u_i]\mu[\delta_x^- u_i]) \\ &\quad - \gamma\delta_x^+(\mu[u_i]\mu[\delta_x^+ u_i]) \Big) \delta[u_i] \\ &= \left\langle \frac{1}{2}\mu[u^2] + \mu[u]^2 + \frac{\gamma}{2}\mu[\delta_x^+ u \delta_x^- u] - \frac{\gamma}{2}\delta_x^-(\mu[u]\mu[\delta_x^- u]) - \frac{\gamma}{2}\delta_x^+(\mu[u]\mu[\delta_x^+ u]), \delta[u] \right\rangle .\end{aligned}$$

Hence,

$$\begin{aligned}\overline{\nabla} H_2(m,m') &= (1-\delta_x^2)^{-1}\big(\frac{1}{2}\mu[u^2] + \mu[u]^2 + \frac{\gamma}{2}\mu[\delta_x^+ u \delta_x^- u] - \frac{\gamma}{2}\delta_x^-(\mu[u]\mu[\delta_x^- u]) \\ &- \frac{\gamma}{2}\delta_x^+(\mu[u]\mu[\delta_x^+ u])\big),\end{aligned} \tag{29}$$

or

$$\begin{aligned}\overline{\nabla} H_2(m,m') &= \frac{1}{4}(1-\delta_x^2)^{-1}\Big(2u^2+2u'^2+2uu'+\gamma(\delta_x^+u\delta_x^-u+\delta_x^+u'\delta_x^-u') \\ &- \frac{\gamma}{2}\delta_x^-\big((u+u')(\delta_x^-u+\delta_x^-u')\big)-\frac{\gamma}{2}\delta_x^+\big((u+u')(\delta_x^+u+\delta_x^+u')\big)\Big). \quad (30)\end{aligned}$$

Note that, if we replace μ by the identity in (27) and (29) (so that the product rule holds exactly) and replace the discrete spatial derivatives by there continuous counterparts, then we obtain $\frac{\delta\mathcal{H}_1}{\delta m}$ and $\frac{\delta\mathcal{H}_2}{\delta m}$, respectively and in this way we check the consistency of the approximation.

Let us now compute the mean value discrete gradient, which we now denote $\overline{\nabla}^m H_j(m,m')$ (for $j=1,2$), as given by (20), that is,

$$\overline{\nabla}^m H_j(m,m') = \int_0^1 \nabla H_j((1-\zeta)m+\zeta m')\mathrm{d}\zeta. \quad (31)$$

Here the gradient ∇H is defined with respect to the discrete scalar product (22) and we have, for all $\tilde{m}$,

$$\begin{aligned}\langle \nabla H_1(m),\tilde{m}\rangle &= \frac{\mathrm{d}}{\mathrm{d}\varepsilon}\Big|_{\varepsilon=0} H_1(m+\varepsilon\tilde{m}) \\ &= \Delta x\sum_{i=0}^{n-1}(u_i\tilde{u}_i+\delta_x^+u_i\delta_x^+\tilde{u}_i) = \Delta x\sum_{i=0}^{n-1}u_i(\tilde{u}_i-\delta_x^2\tilde{u}_i) = \langle u,\tilde{m}\rangle\,,\end{aligned}$$

after one summation by part, so that

$$\nabla H_1(m) = u. \quad (32)$$

In the same way, we obtain

$$\begin{aligned}\langle \nabla H_2(m),\tilde{m}\rangle &= \frac{\mathrm{d}}{\mathrm{d}\varepsilon}\Big|_{\varepsilon=0} H_2(m+\varepsilon\tilde{m}) \\ &= \frac{\Delta x}{2}\sum_{i=0}^{n-1}(3(u_i)^2\tilde{u}_i+\gamma\tilde{u}_i\delta_x^+u_i\delta_x^-u_i+\gamma u_i\delta_x^+\tilde{u}_i\delta_x^-u_i+\gamma u_i\delta_x^+u_i\delta_x^-\tilde{u}_i)\end{aligned}$$

so that

$$\nabla H_2(m) = (1-\delta_x^2)^{-1}\Big(\frac{3}{2}u^2+\frac{\gamma}{2}\delta_x^+u\delta_x^-u-\frac{\gamma}{2}\delta_x^-(u\delta_x^-u)-\frac{\gamma}{2}\delta_x^+(u\delta_x^+u)\Big) \quad (33)$$

(the multiplications are meant component-wise). From (31) and (32), we get

$$\overline{\nabla}^m H_1(m,m') = \int_0^1((1-\zeta)u+\zeta u')\mathrm{d}\zeta = \frac{u+u'}{2}$$

and the mean value discrete gradient coincides with the discrete gradient computed earlier in (28). For the second Hamiltonian, from (31) and (33), we obtain

$$\begin{aligned}
\overline{\nabla}^m H_2(m,m') = (1-\delta_x^2)^{-1}\Big(\int_0^1 \Big(&\tfrac{3}{2}\big((1-\zeta)u+\zeta u'\big)^2 \\
&+\tfrac{\gamma}{2}\big(\delta_x^+((1-\zeta)u+\zeta u')\delta_x^-((1-\zeta)u+\zeta u')\big) \\
&-\tfrac{\gamma}{2}\delta_x^-\big(((1-\zeta)u+\zeta u')(\delta_x^-((1-\zeta)u+\zeta u'))\big) \\
&-\tfrac{\gamma}{2}\delta_x^+\big(((1-\zeta)u+\zeta u')(\delta_x^+((1-\zeta)u+\zeta u'))\big)\Big)\mathrm{d}\zeta\Big) \\
= (1-\delta_x^2)^{-1}\Big(&\tfrac{1}{2}\big(u^2+uu'+u'^2\big)+\tfrac{\gamma}{6}\big(\delta_x^+u\delta_x^-u+\tfrac{1}{2}\delta_x^+u\delta_x^-u' \\
&+\tfrac{1}{2}\delta_x^+u'\delta_x^-u+\delta_x^+u'\delta_x^-u'\big) \\
&-\tfrac{\gamma}{6}\delta_x^-\big(u\delta_x^-u+\tfrac{1}{2}u\delta_x^-u'+\tfrac{1}{2}u'\delta_x^-u+u'\delta_x^-u'\big) \\
&-\tfrac{\gamma}{6}\delta_x^+\big(u\delta_x^+u+\tfrac{1}{2}u\delta_x^+u'+\tfrac{1}{2}u'\delta_x^+u+u'\delta_x^+u'\big)\Big)
\end{aligned} \tag{34}$$

which differs from the discrete gradient computed earlier in (30). It remains to discretize the operators $\mathcal{D}_1$ and $\mathcal{D}_2$. We use the following approximations:

$$D_1(m)(v) = -((u-\gamma\delta_x^2u)\delta_x v) - \delta_x((u-\gamma\delta_x^2u)v) \tag{35}$$

and

$$D_2(m)(v) = -\delta_x(1-\delta_x^2)(v). \tag{36}$$

The choice of discretization of (35) is not unique, see the end of Section 5. Using the summation by part rule (26), it can be checked that the discrete operators D_1 and D_2 are antisymmetric for the discrete scalar product (22). The discrete gradients (28), (30) and (34) are symmetric in m and m', that is, $\overline{\nabla}H(m,m') = \overline{\nabla}H(m',m)$ for any m and m'. For the extensions of the operators D_1 and D_2, we take

$$\tilde{D}_1(m,m',\Delta t)(v) = -((\tfrac{1}{2}(u+u')-\tfrac{\gamma}{2}\delta_x^2(u+u'))\delta_x v) - \delta_x((\tfrac{1}{2}(u+u')-\tfrac{\gamma}{2}\delta_x^2(u+u'))v) \tag{37}$$

and

$$\tilde{D}_2(m,m',\Delta t) = D_2(m), \tag{38}$$

respectively. Note that $\tilde{D}_2(m,m',\Delta t) = D_2(m) = D_2(m')$ because, by definition, $D_2(m)$ does not depend on m. With these special choices, both operators are time independent and so they are symmetric in time, that is,

$$\tilde{D}_j(m,m',\Delta t) = \tilde{D}_j(m',m,-\Delta t) \tag{39}$$

for $j = 1, 2$ and for all m, m', Δt. Finally, we obtain three schemes which all preserve one of the Hamiltonians, see (21). The first scheme is given by

$$\frac{m^{j+1} - m^j}{\Delta t} = \tilde{D}_1(m^{j+1}, m^j, \Delta t)\overline{\nabla} H_1(m^{j+1}, m^j)$$

or, more explicitly,

$$\begin{aligned} u^{j+1} = u^j - \frac{\Delta t}{4}(1-\delta_x^2)^{-1}\Big(&\big(u^{j+1} + u^j - \gamma\delta_x^2(u^{j+1} + u^j)\big)\delta_x(u^{j+1} + u^j) \\ &+ \delta_x\Big(\big(u^{j+1} + u^j - \gamma\delta_x^2(u^{j+1} + u^j)\big)(u^{j+1} + u^j)\Big)\Big). \end{aligned} \tag{40}$$

It preserves the discrete energy H_1. The second scheme is given by

$$\frac{m^{j+1} - m^j}{\Delta t} = D_2(m^j)\overline{\nabla} H_2(m^{j+1}, m^j)$$

or, more explicitly,

$$\begin{aligned} u^{j+1} = u^j - \frac{\Delta t}{4}\delta_x(1-\delta_x^2)^{-1}\Big(&2\big((u^{j+1})^2 + u^{j+1}u^j + (u^j)^2\big) + \gamma(\delta_x^+ u^{j+1}\delta_x^- u^{j+1} + \delta_x^+ u^j \delta_x^- u^j) \\ - \frac{\gamma}{2}\Big(&\delta_x^-\big((u^j + u^{j+1})(\delta_x^- u^j + \delta_x^- u^{j+1})\big) + \delta_x^+\big((u^j + u^{j+1})(\delta_x^+ u^j + \delta_x^+ u^{j+1})\big)\Big)\Big). \end{aligned} \tag{41}$$

The third scheme is given by

$$\frac{m^{j+1} - m^j}{\Delta t} = D_2(m^j)\overline{\nabla}^m H_2(m^{j+1}, m^j)$$

or more explicitly

$$\begin{aligned} u^{j+1} = u^j - \frac{\Delta t}{4}\delta_x(1-\delta_x^2)^{-1}\Big(&2\big((u^{j+1})^2 + u^{j+1}u^j + (u^j)^2\big) \\ &+ \frac{2\gamma}{3}\big(\delta_x^+ u^{j+1}\delta_x^- u^{j+1} + \frac{1}{2}\delta_x^+ u^{j+1}\delta_x^- u^j + \frac{1}{2}\delta_x^- u^{j+1}\delta_x^+ u^j + \delta_x^+ u^j \delta_x^- u^j\big) \\ &- \frac{2\gamma}{3}\delta_x^-\big(u^{j+1}\delta_x^- u^{j+1} + \frac{1}{2}u^{j+1}\delta_x^- u^j + \frac{1}{2}u^j\delta_x^- u^{j+1} + u^j\delta_x^- u^j\big) \\ &- \frac{2\gamma}{3}\delta_x^+\big(u^{j+1}\delta_x^+ u^{j+1} + \frac{1}{2}u^{j+1}\delta_x^+ u^j + \frac{1}{2}u^j\delta_x^+ u^{j+1} + u^j\delta_x^+ u^j\big)\Big). \end{aligned} \tag{42}$$

The schemes (41) and (42) preserve the discrete Hamiltonian H_2. The three schemes are second-order in time since they are symmetric in time by equation (39), see [29].

For the Camassa–Holm equation and the BBM equation, the schemes corresponding to (40) are

$$u^{j+1} = u^j - \frac{\Delta t}{4}(1-\delta_x^2)^{-1}\Big(\big((1-\delta_x^2)(u^{j+1}+u^j)+\kappa\big)\delta_x(u^{j+1}+u^j) + \delta_x\Big(\big((1-\delta_x^2)(u^{j+1}+u^j)+\kappa\big)(u^{j+1}+u^j)\Big)\Big)$$

and

$$u^{j+1} = u^j - \frac{\Delta t}{6}(1-\delta_x^2)^{-1}\Big(\big((u^{j+1}+u^j)\delta_x(u^{j+1}+u^j)\big) + \delta_x\big((u^{j+1})^2+(u^j)^2+2u^{j+1}u^j+3u^{j+1}+3u^j\big)\Big),$$

respectively. For any scalar function, and in particular G, the discrete gradient is unique as we have $\overline{\nabla}G(u,u') = \dfrac{G(u')-G(u)}{u'-u}$. For the generalized hyperelastic-rod wave equation, the schemes (41) and (42) rewrite

$$\begin{aligned} u^{j+1} = u^j - \frac{\Delta t}{4}\delta_x(1-\delta_x^2)^{-1}\Big(&2\overline{\nabla}G(u^{j+1},u^j) \\ &+ \gamma(\delta_x^+u^{j+1}\delta_x^-u^{j+1}+\delta_x^+u^j\delta_x^-u^j) \\ &- \frac{\gamma}{2}\Big(\delta_x^-\big((u^j+u^{j+1})(\delta_x^-u^j+\delta_x^-u^{j+1})\big)+\delta_x^+\big((u^j+u^{j+1})(\delta_x^+u^j+\delta_x^+u^{j+1})\big)\Big)\Big) \end{aligned}$$

and

$$\begin{aligned} u^{j+1} = u^j - \frac{\Delta t}{4}\delta_x(1-\delta_x^2)^{-1}\Big(&2\overline{\nabla}G(u^{j+1},u^j) \\ &+ \frac{2\gamma}{3}\big(\delta_x^+u^{j+1}\delta_x^-u^{j+1}+\frac{1}{2}\delta_x^+u^{j+1}\delta_x^-u^j+\frac{1}{2}\delta_x^-u^{j+1}\delta_x^+u^j+\delta_x^+u^j\delta_x^-u^j\big) \\ &- \frac{2\gamma}{3}\delta_x^-\big(u^{j+1}\delta_x^-u^{j+1}+\frac{1}{2}u^{j+1}\delta_x^-u^j+\frac{1}{2}u^j\delta_x^-u^{j+1}+u^j\delta_x^-u^j\big) \\ &- \frac{2\gamma}{3}\delta_x^+\big(u^{j+1}\delta_x^+u^{j+1}+\frac{1}{2}u^{j+1}\delta_x^+u^j+\frac{1}{2}u^j\delta_x^+u^{j+1}+u^j\delta_x^+u^j\big)\Big). \end{aligned}$$

In the particular cases of the Camassa–Holm equation and the BBM equation, we have

$$\overline{\nabla}G(u,u') = \kappa(u+u')+u^2+u'^2+uu'$$

and

$$\overline{\nabla}G(u,u') = u+u'+\frac{1}{3}(u^2+u'^2+uu'),$$

respectively.

4. Multi-symplectic integrators

We begin this section by reviewing the concept of multi-symplecticity in a general context, for more details, see e.g. [38, 32, 39]. A partial differential equation of the form $F(u, u_t, u_x, u_{tx}, \ldots) = 0$ is said to be *multi-symplectic* if it can be written as a system of first order equations:

$$M\, z_t + K\, z_x = \nabla_z S(z), \tag{43}$$

with $z \in \mathbb{R}^d$ a vector of state variables, typically consisting of the original variable u as one of its components. The matrices M and K are skew-symmetric $d \times d$-matrices, and S is a smooth scalar function depending on z. Equation (43) is not necessarily unique and the dimension d of the state vector may differ from one expression to another. A key observation for the multi-symplectic formulation (43) is that the matrices M and K define symplectic structures on subspaces of $\mathbb{R}^d$,

$$\omega = \mathrm{d}z \wedge M\mathrm{d}z, \qquad \kappa = \mathrm{d}z \wedge K\mathrm{d}z.$$

Considering any pair of solutions to the variational equation associated with (43), we have, see [32], that the following *multi-symplectic conservation law* applies

$$\partial_t \omega + \partial_x \kappa = 0. \tag{44}$$

With the two skew-symmetric matrices M and K, one can also define the density functions

$$\widetilde{E}(z) = S(z) - \frac{1}{2} z_x^T K z\,, \qquad \widetilde{F}(z) = \frac{1}{2} z_t^T K z,$$
$$\widetilde{G}(z) = S(z) - \frac{1}{2} z_t^T M z\,, \qquad \widetilde{I}(z) = \frac{1}{2} z_x^T M z,$$

which immediately yield the *local conservation laws*

$$\partial_t \widetilde{E}(z) + \partial_x \widetilde{F}(z) = 0 \qquad \text{and} \qquad \partial_t \widetilde{I}(z) + \partial_x \widetilde{G}(z) = 0,$$

for any solution to (43). Thus, under the usual assumption on vanishing boundary terms for the functions $\widetilde{F}(z)$ and $\widetilde{G}(z)$ one obtains the globally conserved quantities of (*energy* and *momentum*)

$$\mathcal{E}(z) = \int \widetilde{E}(z)\,\mathrm{d}x \qquad \text{and} \qquad \mathcal{I}(z) = \int \widetilde{I}(z)\,\mathrm{d}x.$$

Since the multi-symplectic conservation law (44) is a *local* conservation law, the multi-symplectic formulation of a partial differential equation may lead to numerical

schemes which render well the local properties of the equation. To derive multi-symplectic integrators, we follow the approach given in [38] (see also [32]) and write the partial differential equation as a system of first order equations (43) and then discretize it. For an alternative construction of multi-symplectic integrators see for example [40].

The main philosophy behind the use of symplectic integrators for Hamiltonian differential equation is that the schemes are designed to preserve the symplectic form of the equation at each time step. For multi-symplectic partial differential equations, the idea of Bridges and Reich [32] was to develop integrators which satisfy a discretized version of the multi-symplectic conservation law (44). For this purpose, they considered a direct discretization of (43), replacing the derivatives with divided differences, and the continuous function $z(t,x)$ by a discrete version $z^{n,i} \approx z(t_i, x_n)$ on a uniform rectangular grid. We set $\Delta x = x_{n+1} - x_n, n \in \mathbb{Z}$, and $\Delta t = t_{i+1} - t_i$, $i \geq 0$ as in Section 3.

Following their notation, we write

$$M\partial_t^{n,i} z^{n,i} + K\partial_x^{n,i} z^{n,i} = \nabla_z S(z^{n,i}), \tag{45}$$

where $\partial_t^{n,i}$ and $\partial_x^{n,i}$ are discretizations of the partial derivatives ∂_t and ∂_x, respectively. A natural way of inferring multi-symplecticity on the discrete level is to demand that for any pairs $(U^{n,i}, V^{n,i})$ of solutions to the corresponding variational equation of (45), one has

$$\partial_t^{n,i}\omega_{n,i} + \partial_x^{n,i}\kappa_{n,i} = 0,$$

where

$$\omega_{n,i}(U^{n,i}, V^{n,i}) = \langle MU^{n,i}, V^{n,i}\rangle, \qquad \kappa_{n,i}(U^{n,i}, V^{n,i}) = \langle KU^{n,i}, V^{n,i}\rangle,$$

with the Euclidean scalar product $\langle\cdot,\cdot\rangle$ on $\mathbb{R}^d$.

As for the Camassa-Holm equation, see [24], setting $z = [u, \phi, w, v, \nu]^T$, we derive the following multi-symplectic formulation (43) for the generalized hyperelastic-rod wave equation (1):

$$\begin{pmatrix} 0 & 1/2 & 0 & 0 & -1/2 \\ -1/2 & 0 & 0 & 0 & 0 \\ 0 & 0 & 0 & 0 & 0 \\ 0 & 0 & 0 & 0 & 0 \\ 1/2 & 0 & 0 & 0 & 0 \end{pmatrix} z_t + \begin{pmatrix} 0 & 0 & 0 & -1 & 0 \\ 0 & 0 & 1 & 0 & 0 \\ 0 & -1 & 0 & 0 & 0 \\ 1 & 0 & 0 & 0 & 0 \\ 0 & 0 & 0 & 0 & 0 \end{pmatrix} z_x = \begin{pmatrix} -w - \frac{1}{2}g(u) - \gamma\frac{\nu^2}{2} \\ 0 \\ -u \\ \nu \\ -\gamma u\nu + v \end{pmatrix}, \tag{46}$$

with the scalar function $S(z) = -wu - \frac{1}{2}G(u) - \gamma u\frac{\nu^2}{2} + v\nu$, recalling $G(u) := \int g(u)$. In [24], two multi-symplectic formulations are derived for the Camassa–Holm equation. The second one is based on a reformulation of the equation which takes into account the energy as an additional variable. This reformulation, which can handle peakon-antipeakon collisions, is inspired from [41] and it has been extended to the generalized hyperelastic-rod wave equation in [2]. We tried hard but did not succeed to extend the second multi-symplectic formulation of [24] to the hyperelastic-rod wave equation. This difficulty may reflect the fact that the Camassa–Holm equation enjoys a much richer mathematical structure than the hyperelastic-rod wave equation (Lax pair, complete integrability, geodesic equation, etc ...)

We now turn to the calculation of the global invariants (energy and momentum) defined above. For the hyperelastic-rod wave equation, an integration of the conservation law $\partial_t \widetilde{I}(z) + \partial_x \widetilde{G}(z) = 0$ leads to:

$$\frac{1}{4}\frac{\mathrm{d}}{\mathrm{d}t}\int \big(-u_x\phi + u_x^2 + u^2 - uu_{xx}\big)\mathrm{d}x + \big[\widetilde{G}(z)\big] = 0,$$

where the brackets stand for the difference of the function evaluated at the upper and lower limit of the integral. As in [24], after an integration by parts on the first and last term, using periodic (or vanishing at infinity) boundary conditions of u (i.e. $[u] = [u_x] = [u_{xx}] = [\phi_t] = 0$), we obtain the following global invariant for the hyperelastic-rod wave equation:

$$\mathcal{I} = \frac{1}{2}\int (u^2 + u_x^2)\mathrm{d}x.$$

Similarly, the second conservation law $\partial_t \widetilde{E}(z) + \partial_x \widetilde{F}(z) = 0$ leads to

$$\mathcal{E} = -\frac{1}{2}\int (u^3 + \gamma u u_x^2)\mathrm{d}x.$$

We remark that these two conserved quantities are (up to a multiplicative constant) the Hamiltonian functionals given in (9)-(10).

The Euler box scheme. By taking the splitting $M = M_+ + M_-$ with $M_+ = M_- = \frac{1}{2}M$ (and similarly for K) we obtain the Euler-box scheme, a multi-symplectic integrator for the generalized hyperelastic-rod wave equation, expressed in terms of u (see [24]

and [39]):

$$
\begin{aligned}
- \quad & 4\Delta x^2 u^{n,i+1} + \big(u^{n+2,i+1} - 2u^{n,i+1} + u^{n-2,i+1}\big) = \\
8 \quad & \Delta x^2 \Delta t \Big\{ -\frac{1}{2\Delta t} u^{n,i-1} - \frac{1}{2\Delta x}\Big(-\frac{1}{2} g(u^{n+1,i}) + \frac{1}{2} g(u^{n-1,i}) - \frac{\gamma}{8\Delta x^2}(u^{n+2,i} - u^{n,i})^2 \\
+ \quad & \frac{\gamma}{8\Delta x^2}(u^{n,i} - u^{n-2,i})^2 + \frac{1}{4\Delta x \Delta t}(-u^{n+2,i-1} + 2u^{n,i-1} - u^{n-2,i-1}) \\
+ \quad & \frac{\gamma}{4\Delta x^2}(u^{n+2,i}(u^{n+3,i} - u^{n+1,i}) - 2u^{n,i}(u^{n+1,i} - u^{n-1,i}) + u^{n-2,i}(u^{n-1,i} - u^{n-3,i}))\Big)\Big\}.
\end{aligned}
$$

Equation (1) can be rewritten in the form

$$
u_t - u_{xxt} + \big(\frac{1}{2} g(u) + \frac{\gamma}{2} u_x^2\big)_x - \gamma (u u_x)_{xx} = 0 \tag{47}
$$

and the corresponding Euler-box scheme is given in a more compact form by

$$
\delta_t u^{n,i} - \delta_x \delta_x \delta_t u^{n,i} + \delta_x \big(\frac{1}{2} g(u^{n,i}) + \frac{\gamma}{2}(\delta_x u^{n,i})^2\big) - \gamma \delta_x \delta_x (u^{n,i} \delta_x u^{n,i}) = 0, \tag{48}
$$

recalling from Section 3 the definitions of the centered differences $\delta_x = \frac{1}{2}(\delta_x^+ + \delta_x^-)$ and, similarly in time, $\delta_t = \frac{1}{2}(\delta_t^+ + \delta_t^-)$. Note that this scheme is only linearly implicit.

Before closing this section, we would like to mention that we only consider the Euler box scheme for the sake of simplicity. We have implemented the Preissman box scheme with Newton's method. However, the Jacobian matrix is ill conditioned so that we cannot use this box scheme.

5. Numerical experiments

In this section, we present numerical experiments. We focus on the the hyperelastic-rod wave equation (3) and present one test for the BBM equation. The results for the Camassa–Holm equation (that is $\gamma = 1$) do not essentially differ from those for the hyperelastic-rod wave equation. We will consider two types of initials conditions: A smooth traveling wave and a single peakon.

5.1. Initial data

This two types of initial conditions are obtained in the following way (see [42, 43] for a derivation of all the traveling wave of (3)). Looking at the Hamiltonian formulation of (3) with (9), we define

$$
v = u - \gamma u_{xx}
$$

so that $m = \frac{\gamma-1}{\gamma}u + \frac{v}{\gamma}$ and the partial differential equation becomes

$$\frac{1}{\gamma}((\gamma-1)u_t + v_t) + (vu)_x + vu_x = 0. \tag{49}$$

For a traveling wave with speed c, we have

$$u(t,x) = U(x-ct) \text{ and } v(t,x) = V(x-ct)$$

and (49) yields

$$-\frac{c}{\gamma}((\gamma-1)U' + V') + V'U + 2VU' = 0.$$

Thus,

$$(U - \frac{c}{\gamma})V' + 2U'(V - \frac{c}{2\gamma}(\gamma-1)) = 0. \tag{50}$$

After multiplying both sides of (50) by $(U - \frac{c}{\gamma})$, we get

$$(U - \frac{c}{\gamma})^2 V' + 2U'(U - \frac{c}{\gamma})(V - \frac{c}{2\gamma}(\gamma-1)) = 0$$

which can be integrated and gives

$$(V - \frac{c}{2\gamma}(\gamma-1))(U - \frac{c}{\gamma})^2 = \alpha \tag{51}$$

for some constant α. Using the fact that $V = U - \gamma U''$, we can rewrite (51) and obtain

$$U'' = -\frac{c(\gamma-1)}{2\gamma^2} + \frac{1}{\gamma}U - \frac{\alpha\gamma}{(\gamma U - c)^2} \tag{52}$$

which is a second order equation for the traveling wave U. After multiplying (52) by U' and integrating one more time we recover the equations given in [42, 43]. However, (52) is easier to implement numerically. We use equation (52) to derive the equations of the smooth traveling wave and the peakon. For the BBM equation, a simple computation gives us that the traveling wave $u(t,x) = U(x-ct)$ satisfies

$$cU'' = (c-1)U - \frac{1}{2}U^2 + \alpha \tag{53}$$

where α is an integrating constant. Note that, if u is a solution of the BBM equation (4), then $\bar{u}(t,x) = u(\frac{t}{3}, x) + 1$ is a solution to the hyperelastic-rod wave equation for $\gamma = 0$ so that the numerical schemes derived for the hyperelastic-rod wave equation can in practice be also used directly for the BBM equation.

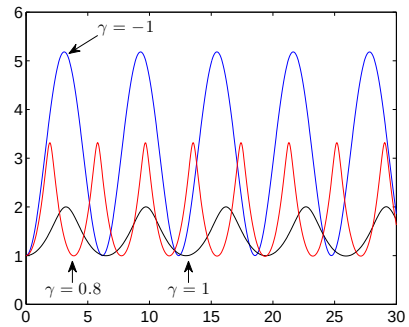

Figure 1: Smooth traveling waves for the hyperelastic-rod wave equation for different values of γ.

Smooth traveling wave: We do not obtain smooth traveling waves for all the values of the parameters α, c and γ. For $c = \alpha = 3$, we solve numerically (52) with initial data $U(0) = 1$ and $U'(0) = 0$. We use the solver `ode45` from matlab with high accuracy. The results are presented in Figure 1 for different values of γ.

Single peakon: Taking $\alpha = 0$ in (52), we obtain the peakons. Indeed, on the line, the general solution of this second order differential equation is given by

$$U(\zeta) = \frac{c(\gamma-1)}{2\gamma} + A\mathrm{e}^{-\zeta/\sqrt{\gamma}} + B\mathrm{e}^{\zeta/\sqrt{\gamma}},$$

for some constants A and B. As it is noted in [43], a traveling wave can only have a point of discontinuity ζ_0 when U reaches the value $\frac{c}{\gamma}$, that is, $U(\zeta_0) = \frac{c}{\gamma}$. For a single peakon, there is only one point of discontinuity ζ_0 (the top of the peak) and we impose $\zeta_0 = 0$. To obtain vanishing at infinity boundary conditions, we must have $A = B$ and thus

$$U(\zeta) = \frac{c}{\gamma}\big(\frac{\gamma-1}{2} + (1 - \frac{\gamma-1}{2})\mathrm{e}^{-|\zeta|/\sqrt{\gamma}}\big)$$

so that, on the line, the peakon-solution of the hyperelastic-rod wave equation is then given by

$$u(t,x) = \frac{c}{2\gamma}\big(\gamma - 1 + (3-\gamma)\mathrm{e}^{-|x-ct|/\sqrt{\gamma}}\big).$$

Still for $\alpha = 0$, by choosing the points of discontinuity at $-T/2$ and $T/2$, we obtain the periodic peakon. On the interval $[-T/2, T/2]$, this gives

$$U(\zeta) = \frac{c}{2\gamma}\big(\gamma - 1 + \frac{(3-\gamma)}{\cosh(T/(2\sqrt{\gamma}))}\cosh(\frac{\zeta}{\sqrt{\gamma}})\big),$$

so that the periodic peakon is

$$u(t,x) = \frac{c}{2\gamma}\Big(\gamma - 1 + \frac{(3-\gamma)}{\cosh(T/(2\sqrt{\gamma}))}\cosh\Big(\frac{d(x-ct)}{\sqrt{\gamma}}\Big)\Big), \tag{54}$$

for $d(x) = \bar{x} - \frac{T}{2}$ where $\bar{x}$ is the unique element of $[0, T)$ for which there exists $k \in \mathbb{Z}$ such that $\bar{x} = x + \frac{T}{2} + kT$.

5.2. Simulations

Before we proceed with the numerical experiments, let us give some remarks concerning implementation issues. For the multi-symplectic scheme (48) applied to equation (3), the first needed step for the iteration will be computed along the exact solution of the problem. The integrals in the Hamiltonians given in (9) and (10) will be discretized in such a way that we obtain the conserved quantities (24), resp. (25) from the energy-preserving schemes (40), (41) and (42). All the numerical experiments will be done for the hyperelastic-rod wave equation with the constant $\gamma = 0.8$. The smooth traveling wave considered will be the solution of (52) with $c = \alpha = 3$. In this case we obtain a period $T \approx 3.8609$ for the traveling wave. For the single peakon (54), we take $T = 40$ and $c = 1$. In the following figures, we will denote by *scheme MS*, *scheme 1*, *scheme 2*, resp. *scheme 3* the multi-symplectic scheme, and the schemes (40), (41), (42).

We first consider the temporal rate of convergence of our schemes. We vary the time step Δt and set the space step to $\Delta x = c\,\Delta t/0.9$. One can see from Figure 2 that the order of convergence is two for the smooth solution and one for the non-smooth one, and this holds for all the schemes. Similar behavior are also observed for the spatial rate of convergence of the numerical methods: order one for the non-smooth solution and order two for the smooth one. The results are however not displayed. We next take a fixed small time step $\Delta t = 0.01$ and varies the space step Δx. The rate of convergence of our schemes are shown on Figure 3. Again, order two, resp. order one is observed for all the schemes.

We next plot the discretizations (24) and (25) of the Hamiltonian functionals of our problem. For the smooth solutions, the grid parameters are $\Delta x = 0.04$ and $\Delta t = 0.01$. For the single peakon solution, they are given by $\Delta x = 0.13$ and $\Delta t = 0.01$. The integrations are done over the time interval $[0, 5]$. Figures 4 and 5 display the results for the discretization of the Hamiltonians given by (24) and (25), respectively. For the non-smooth solution, we also integrate the problem over a longer time intervall ($[0, 10]$) and notice that the multi-symplectic scheme and scheme (40) perfom better than the others. However, on a short time intervall ($[0, 5]$ again), we were able to use much larger time steps (ten times larger, in fact) for the energy preserving schemes compared with the multi-symplectic scheme. For the smooth solution all schemes perform well.

We now look at the Hamiltonian functionals of the BBM equation (4). Figure 6 displays the results for the smooth solution (53) to the BBM equation (we take

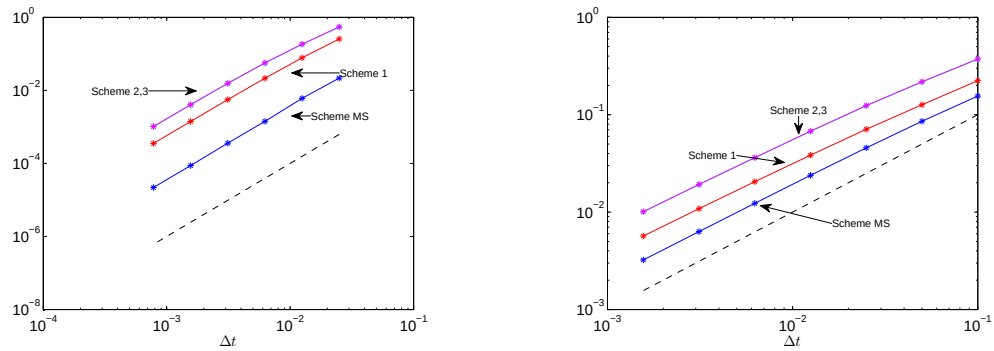

Figure 2: L^2-error of the schemes (40), (41), (42) and (48) at time $Tend = 2$ for the smooth solution (left) and for the peakon (right). The dashed lines have slopes two, resp. one.

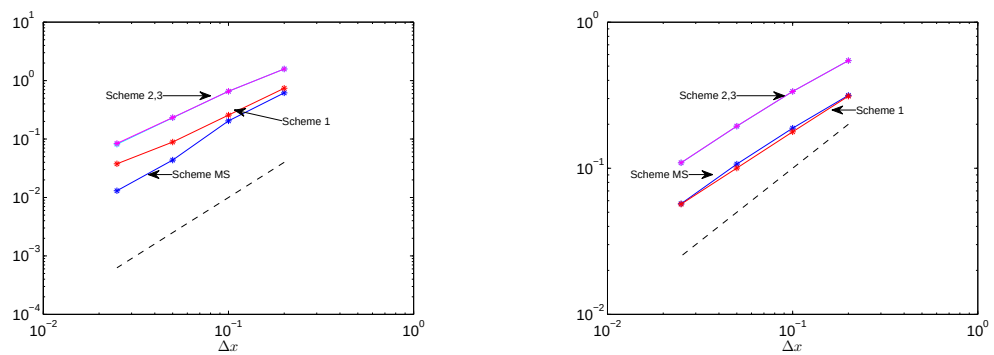

Figure 3: L^2-error of the schemes (40), (41), (42) and (48) at time $Tend = 2$ with a fixed $\Delta t = 0.01$ for the smooth solution (left) and for the peakon (right). The dashed lines have slopes two, resp. one.

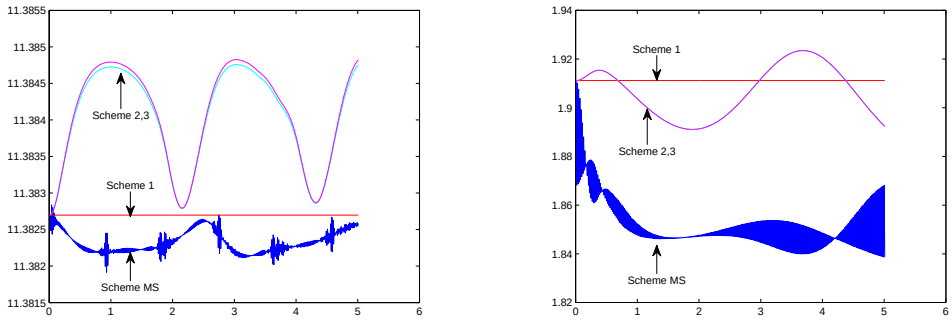

Figure 4: The Hamiltonian (24) along the numerical solutions given by the schemes (40), (41), (42) and (48) for the smooth (left) and non-smooth (right) solution.

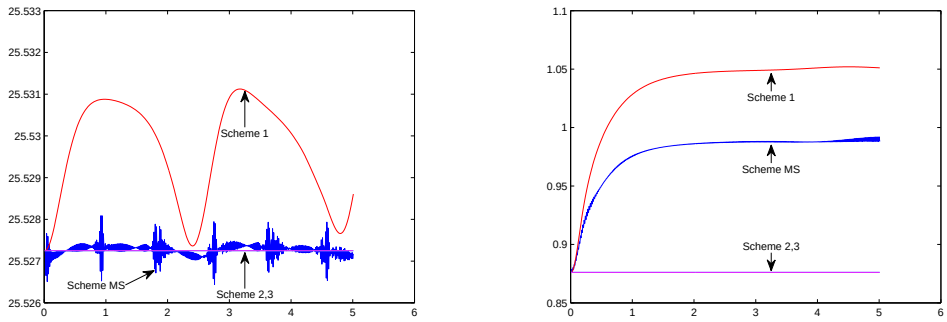

Figure 5: The Hamiltonian (25) along the numerical solutions given by the schemes (40), (41), (42) and (48) for the smooth (left) and non-smooth (right) solution.

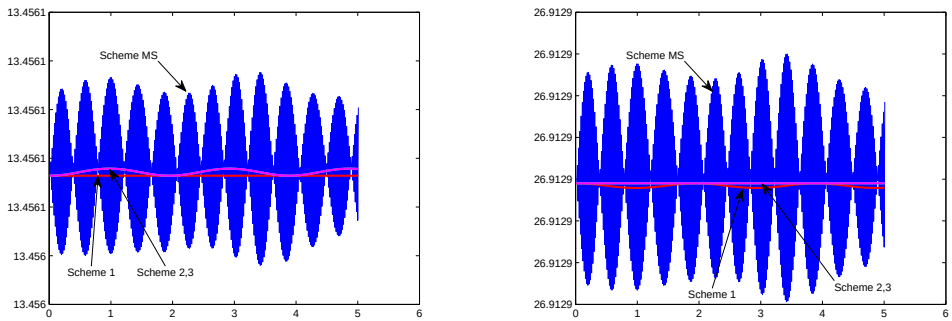

Figure 6: The Hamiltonian (24) (left) and (25) (right) along the numerical solutions given by the schemes (40), (41), (42) and (48) for the smooth solution to the BBM equation.

$\alpha = 0$) with step sizes $\Delta t = 0.01$ and $\Delta x = 0.07$.

Next, we look at the convergence rates for the two Hamiltonians (24) and (25). Figure 7 shows the relative errors in these conserved quantities for the smooth traveling wave. Once again, we vary the time step Δt and set the space step to $\Delta x = c\ \Delta t/0.9$. The integrations are done over the time interval $[0, 2]$. We remark that the order of convergence of the schemes is three. Thus, the convergence towards the Hamiltonians occurs faster than the convergence of the L^2-error, which has an order of convergence equal to two (see Figure 2). We also compare the convergence rate in the conserved quantities for the peakon solution and observe an order of convergence of one. The results are displayed on Figure 8.

Finally, we take again a (small) fixed time step $\Delta t = 0.005$ and let Δx varies. The convergence rate in the conserved quantities are displayed on Figure 9 and Figure 10. The same order of convergence as above is observed.

5.3. Discussions

From our numerical experiments, we can see that the error for the multi-symplectic scheme is in many cases relatively smaller compared to the other schemes. However, the schemes seem otherwise to perform in a comparable manner and in particular it is not clear if one can take advantage of the global or local nature of the schemes (global for the schemes (40), (41), (42) as they preserve one of the Hamiltonians, or local for the multi-symplectic scheme (48)).

Finally, we would like to comment about the degree of freedom we have when deriving the schemes that have been presented. We already saw that the discrete gradient of a function is not unique and presented two ways of computing it. In

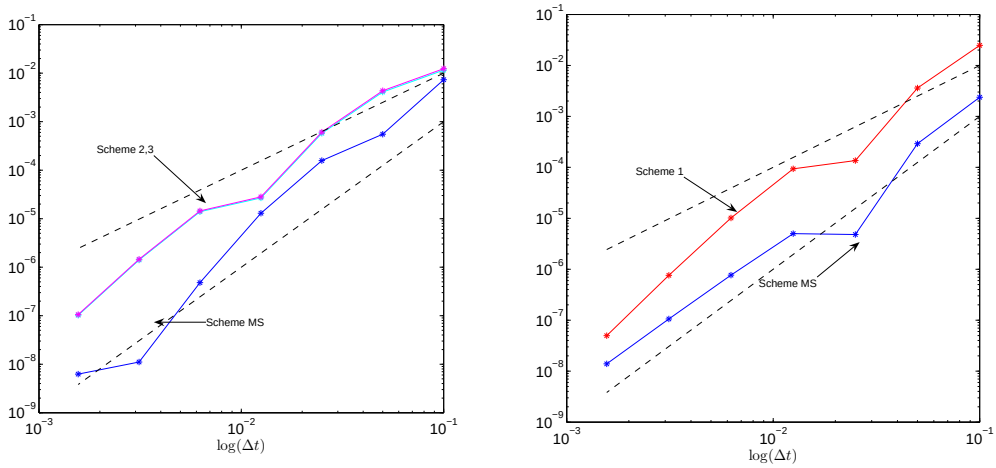

Figure 7: Convergence rates for the Hamiltonians (24) (left) and (25) (right). The numerical solutions are given by the schemes (40), (41), (42) and (48) for the smooth solution. The dashed lines have slopes two and three.

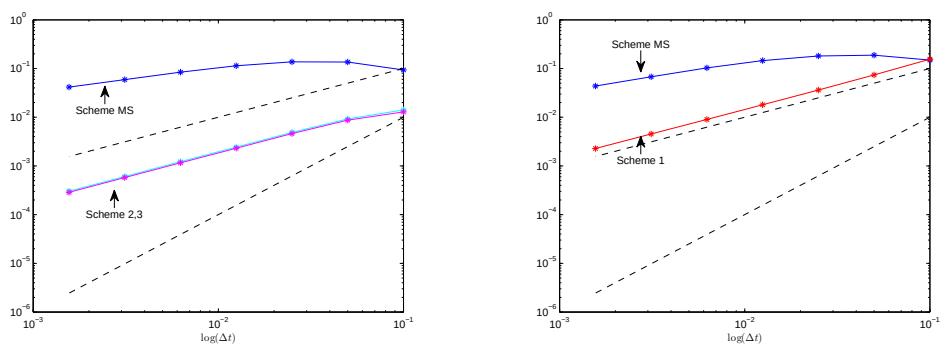

Figure 8: Convergence rates for the Hamiltonians (24) (left) and (25) (right). The numerical solutions are given by the schemes (40), (41), (42) and (48) for the peakon solution. The dashed lines have slopes one and two.

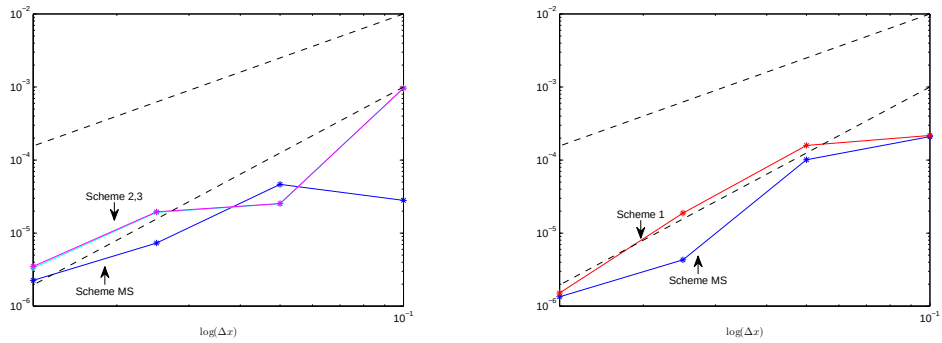

Figure 9: Convergence rates for the Hamiltonians (24) (left) and (25) (right). The numerical solutions are given by the schemes (40), (41), (42) and (48) for the smooth solution with a fixed time step $\Delta t = 0.005$. The dashed lines have slopes two and three.

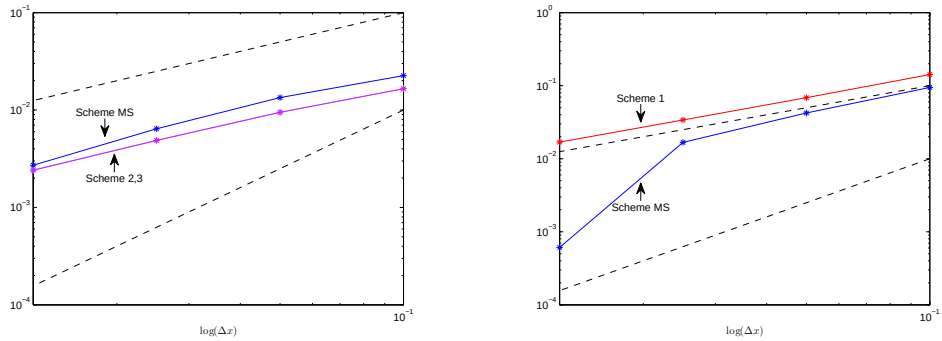

Figure 10: Convergence rates for the Hamiltonians (24) (left) and (25) (right). The numerical solutions are given by the schemes (40), (41), (42) and (48) for the peakon solution with a fixed time step $\Delta t = 0.005$. The dashed lines have slopes one and two.

addition, when discretizing the antisymmetric operators $\mathcal{D}_1$, we used the symmetric discrete derivative δ. We could have used instead left and right discrete derivatives and obtain schemes with the same preserving property. For example, instead of (35), we can take

$$D_1(m)(v) = -((u - \gamma\delta_x^2 u)\delta_x^- v) - \delta_x^+((u - \gamma\delta_x^2 u)v). \tag{55}$$

By using the discrete summation by part rule (23), we can check that this operator is antisymmetric and, in the same way as we derived from (35) the numerical scheme (40), we can obtain from (55) a numerical scheme that *exactly* preserves the discrete Hamiltonian H_1. We have implemented this particular scheme and observed that it may be very unstable, for example in the case of a smooth wave (traveling from left to right) as initial data. This bad behavior is due to the discrete difference operator δ_x^+ in (55), which models the transport of the momentum $u - \gamma u_{xx}$ at a speed u. In the case we are looking at, the "information" is traveling in the same direction as the wave, from left to right, but the right discrete derivative δ_x^+ compute the difference by taking values from the opposite direction, from the right. We can observe that, if we consider as initial data a wave now traveling from right to left, the same scheme performs well. This confirms the stabilizing effect of the symmetric discrete derivative and justifies its use. It also shows that the preservation of energy alone does not guarantee the well-behavior of a scheme.

6. Acknowledgment

We would like to thank Ernst Hairer and Brynjulf Owren for interesting discussions. We appreciate the constructive referees' comments on an earlier version.

[1] G. M. Coclite, H. Holden, K. H. Karlsen, Global weak solutions to a generalized hyperelastic-rod wave equation, SIAM J. Math. Anal. 37 (4) (2005) 1044–1069 (electronic).

[2] H. Holden, X. Raynaud, Global conservative solutions of the Camassa–Holm equation—a Lagrangian point of view, Comm. Partial Differential Equations 32 (10-12) (2007) 1511–1549.

[3] R. Camassa, D. D. Holm, An integrable shallow water equation with peaked solitons, Phys. Rev. Lett. 71 (11) (1993) 1661–1664.

[4] A. Constantin, On the scattering problem for the Camassa–Holm equation, R. Soc. Lond. Proc. Ser. A Math. Phys. Eng. Sci. 457 (2008) (2001) 953–970.

[5] A. Constantin, J. Lenells, On the inverse scattering approach to the Camassa–Holm equation, J. Nonlinear Math. Phys. 10 (3) (2003) 252–255.

[6] D. J. Kaup, Evolution of the scattering coefficients of the Camassa-Holm equation, for general initial data, Stud. Appl. Math. 117 (2) (2006) 149–164.

[7] S. Kouranbaeva, The Camassa–Holm equation as a geodesic flow on the diffeomorphism group, J. Math. Phys. 40 (2) (1999) 857–868.

[8] A. Constantin, B. Kolev, Geodesic flow on the diffeomorphism group of the circle, Comment. Math. Helv. 78 (4) (2003) 787–804.

[9] H.-H. Dai, Exact travelling-wave solutions of an integrable equation arising in hyperelastic rods, Wave Motion 28 (4) (1998) 367–381.

[10] A. Constantin, W. A. Strauss, Stability of a class of solitary waves in compressible elastic rods, Phys. Lett. A 270 (3-4) (2000) 140–148.

[11] Z. Yin, On the Cauchy problem for a nonlinearly dispersive wave equation, J. Nonlinear Math. Phys. 10 (1) (2003) 10–15.

[12] T. B. Benjamin, J. L. Bona, J. J. Mahony, Model equations for long waves in nonlinear dispersive systems, Philos. Trans. Roy. Soc. London Ser. A 272 (1220) (1972) 47–78.

[13] A. Constantin, J. Escher, Wave breaking for nonlinear nonlocal shallow water equations, Acta Math. 181 (2) (1998) 229–243.

[14] A. Constantin, J. Escher, Well-posedness, global existence, and blowup phenomena for a periodic quasi-linear hyperbolic equation, Comm. Pure Appl. Math. 51 (5) (1998) 475–504.

[15] R. Camassa, D. D. Holm, J. Hyman, A new integrable shallow water equation, Adv. Appl. Mech. 31 (1994) 1–33.

[16] H. Kalisch, J. Lenells, Numerical study of traveling-wave solutions for the Camassa–Holm equation, Chaos Solitons Fractals 25 (2) (2005) 287–298.

[17] R. Camassa, J. Huang, L. Lee, Integral and integrable algorithms for a nonlinear shallow-water wave equation, J. Comput. Phys. 216 (2) (2006) 547–572.

[18] R. Camassa, J. Huang, L. Lee, On a completely integrable numerical scheme for a nonlinear shallow-water wave equation, J. Nonlinear Math. Phys. 12 (suppl. 1) (2005) 146–162.

[19] H. Holden, X. Raynaud, A numerical scheme based on multipeakons for conservative solutions of the Camassa–Holm equation, in: Hyperbolic problems: theory, numerics, applications, Springer, Berlin, 2008, pp. 873–881.

[20] H. Holden, X. Raynaud, A convergent numerical scheme for the Camassa–Holm equation based on multipeakons, Discrete Contin. Dyn. Syst. 14 (3) (2006) 505–523.

[21] G. M. Coclite, K. H. Karlsen, N. H. Risebro, A convergent finite difference scheme for the Camassa–Holm equation with general H^1 initial data., SIAM J. Numer. Anal. 46 (3) (2008) 1554–1579 (electronic).

[22] H. Holden, X. Raynaud, Convergence of a finite difference scheme for the Camassa–Holm equation, SIAM J. Numer. Anal. 44 (4) (2006) 1655–1680 (electronic).
URL `http://link.aip.org/link/?SNA/44/1655/1`

[23] Y. Xu, C.-W. Shu, A local discontinuous Galerkin method for the Camassa–Holm equation, SIAM J. Numer. Anal., to appear.

[24] D. Cohen, B. Owren, X. Raynaud, Multi-symplectic integration of the Camassa-Holm equation, Jour. Comp. Phys. 227 (11) (2008) 5492–5512.

[25] T. Wang, L. Zhang, New conservative schemes for regularized long wave equation, Numer. Math. J. Chin. Univ. (Engl. Ser.) 15 (4) (2006) 348–356.

[26] J. Lin, Z. Xie, J. Zhou, High-order compact difference scheme for the regularized long wave equation, Comm. Numer. Methods Engrg. 23 (2) (2007) 135–156.

[27] S. Kutluay, A. Esen, A finite difference solution of the regularized long-wave equation, Math. Probl. Eng. (2006) Art. ID 85743, 14.

[28] T. Matsuo, H. Yamaguchi, An energy-conserving galerkin scheme for a class of nonlinear dispersive equations, Journal of Computational Physics 228 (12) (2009) 4346 – 4358. doi:DOI: 10.1016/j.jcp.2009.03.003.
URL `http://www.sciencedirect.com/science/article/B6WHY-4VTKKXJ-2/2/2f32d8bf72dbfbffa7e736402145e2c6`

[29] R. I. McLachlan, G. R. W. Quispel, N. Robidoux, Geometric integration using discrete gradients, R. Soc. Lond. Philos. Trans. Ser. A Math. Phys. Eng. Sci. 357 (1754) (1999) 1021–1045.

[30] D. Furihata, Finite-difference schemes for nonlinear wave equation that inherit energy conservation property, J. Comput. Appl. Math. 134 (1-2) (2001) 37–57.

[31] T. Matsuo, D. Furihata, Dissipative or conservative finite-difference schemes for complex-valued nonlinear partial differential equations, J. Comput. Phys. 171 (2) (2001) 425–447.

[32] T. J. Bridges, S. Reich, Multi-symplectic integrators: numerical schemes for Hamiltonian PDEs that conserve symplecticity, Phys. Lett. A 284 (4-5) (2001) 184–193.

[33] O. Gonzalez, Time integration and discrete Hamiltonian systems, J. Nonlinear Sci. 6 (5) (1996) 449–467.

[34] P. J. Olver, Applications of Lie groups to differential equations, 2nd Edition, Vol. 107 of Graduate Texts in Mathematics, Springer-Verlag, New York, 1993.

[35] A. Constantin, The Hamiltonian structure of the Camassa-Holm equation, Exposition. Math. 15 (1) (1997) 53–85.

[36] A. Harten, P. D. Lax, B. van Leer, On upstream differencing and Godunov-type schemes for hyperbolic conservation laws, SIAM Rev. 25 (1) (1983) 35–61.

[37] U. M. Ascher, Numerical methods for evolutionary differential equations, Vol. 5 of Computational Science & Engineering, Society for Industrial and Applied Mathematics (SIAM), Philadelphia, PA, 2008.

[38] T. J. Bridges, Multi-symplectic structures and wave propagation, Math. Proc. Cambridge Philos. Soc. 121 (1) (1997) 147–190.

[39] B. Moore, S. Reich, Backward error analysis for multi-symplectic integration methods, Numer. Math. 95 (4) (2003) 625–652.

[40] J. E. Marsden, G. W. Patrick, S. Shkoller, Multisymplectic geometry, variational integrators, and nonlinear PDEs, Comm. Math. Phys. 199 (2) (1998) 351–395.

[41] H. Holden, X. Raynaud, Global conservative solutions of the generalized hyperelastic-rod wave equation, J. Differential Equations 233 (2) (2007) 448–484.

[42] H.-H. Dai, Y. Huo, Solitary shock waves and other travelling waves in a general compressible hyperelastic rod, R. Soc. Lond. Proc. Ser. A Math. Phys. Eng. Sci. 456 (1994) (2000) 331–363.

[43] J. Lenells, Traveling waves in compressible elastic rods, Discrete Contin. Dyn. Syst. Ser. B 6 (1) (2006) 151–167 (electronic).